This article may be used for research, teaching, and private study purposes. Any substantial or systematic reproduction, redistribution, reselling, loan, sub-licensing, systematic supply, or distribution in any form to anyone is expressly forbidden.

The publisher does not give any warranty express or implied or make any representation that the contents will be complete or accurate or up to date. The accuracy of any instructions, formulae, and drug doses should be independently verified with primary sources. The publisher shall not be liable for any loss, actions, claims, proceedings, demand, or costs or damages whatsoever or howsoever caused arising directly or indirectly in connection with or arising out of the use of this material.

Downloaded by [USP University of Sao Paulo] at 08:21 30 April 2013

International Journal of Remote Sensing
Vol. 26, No. 13, 10 July 2005, 2797–2816

Taylor & Francis
Taylor & Francis Group

Tropospheric aerosol observations in São Paulo, Brazil using a compact lidar system

E. LANDULFO*†, A. PAPAYANNIS‡, A. Z. DE FREITAS†, N. D. VIEIRA JR†, R. F. SOUZA†, A. GONÇALVES†, A. D. A. CASTANHO§, P. ARTAXO§, O. R. SÁNCHEZ-CCOYLLO¶, D. S. MOREIRA¶ and M. P. M. P. JORGE**

†Instituto de Pesquisas Energéticas e Nucleares, Centro de Lasers e Aplicações Avenida Lineu Prestes, 2242 Cidade Universitária, CEP 05508-900, São Paulo, SP, Brazil

‡National Technical University of Athens, Heroon Polytechniou 9, 15780 Zografou, Greece

§Instituto de Física, Universidade de São Paulo, Rua do Matão, Travessa R 187, CEP 05508-901, São Paulo, SP, Brazil

¶Instituto de Astronomia, Geofísica, e Ciências Atmosféricas, Universidade de São Paulo, Departamento de Ciências Atmosféricas, Rua do Matão 1226, CEP 05508-900, São Paulo, SP, Brazil

**Laboratório Associado de Meteorologia e Oceanografia, Centro de Previsão do Tempo e Estudos Climáticos, Instituto Nacional de Pesquisas Espaciais, Av. dos Astronautas 1758, CEP 12201-970, Sao José dos Campos, SP, Brazil

(*Received 10 January 2003; in final form 1 November 2004*)

A backscattering light detection and ranging (lidar) system, the first of this kind in the country, has been set up in a suburban area in the city of São Paulo, Brazil (23°33′ S, 46°44′ W) to provide the vertical profile of the aerosol backscatter and extinction coefficients at 532 nm and up to 4–5 km height above sea level (asl). The measurements have been carried out during the second half of the so-called Brazilian dry season, September and October in the year of 2001. When possible, the lidar measurements were complemented with aerosol optical thickness measurements obtained by a CIMEL Sun-tracking photometer in the visible spectral region, not only to validate the lidar data, but also to provide an input value of the so-called extinction-to-backscatter ratio (lidar ratio). The lidar data were also used to retrieve the Planetary Boundary Layer (PBL) height and low troposphere structural features over the city of São Paulo. Three-dimensional air mass back trajectory analysis was also conducted to determine the source regions of aerosols observed during this study. These first lidar measurements over the city of São Paulo during the second half of the dry season showed a significant variability of the aerosol optical thickness (AOT) in the lower troposphere (0.5–5 km) at 532 nm. It was also found that the aerosol load is maximized in the 1–3 km height region and this load represents about 20–25% of the lower tropospheric aerosol.

1. Introduction

Air pollution in mega cities is one of the most important problems of our era. The city of São Paulo is in the rank of the five largest metropolitan areas of the world, as

*Corresponding author. Email: elandulf@net.ipen.br; fax: 55 11 38169315

International Journal of Remote Sensing
ISSN 0143-1161 print/ISSN 1366-5901 online © 2005 Taylor & Francis Group Ltd
http://www.tandf.co.uk/journals
DOI: 10.1080/01431160500033971

Downloaded by [USP University of Sao Paulo] at 08:21 30 April 2013

well as one of the most populated areas having about 17 million inhabitants. Therefore, in all these mega-cities the human activities have an enormous impact on the local atmosphere, as well as on their population health (Saldiva *et al.* 1995, Macchione *et al.* 1999). Concerning the atmospheric quality, we highlight the suspended aerosol particles as a subject of continuous interest (Pandis *et al.* 1995) due to the ongoing expansion of the metropolitan area, which carries more than 3000 industries. Among them the main aerosol sources include heavy industries, such as iron- and steelworks, refineries, chemical manufacturing, cement, sulphuric acid, petrochemical plants, and the automotive fleet, the latter exceeding already 5 million vehicles.

Regarding its topography the city is located in a plateau at about 800 m above sea level (asl) and is surrounded by hills of about 1200 m high. During the summer season the precipitation increases and many cold fronts generate meteorological instabilities, which indeed favour the pollution dispersion. These periods can extend over the autumn months of May and June; later on when the wintertime begins, a high-pressure semi-static regime over the São Paulo area is generally observed. This event becomes highly favourable to pollutants accumulation, especially during episodes of intense temperature inversions, occurring typically at 1000 m asl (Alonso *et al.* 1997).

To extend the comprehension of the scenery described above a multi-instrument approach could be extremely helpful. Many studies of the vertical profile of the tropospheric aerosol load have been conducted using the light detection and ranging (lidar) technique not only in the European continent (Boesenberg *et al.* 2001, 2003) and North America but also in some Asian countries (Bissonnette *et al.* 2002). Despite its simple conception, its design and technologies are complex, and it has become a useful tool in meteorology, in atmospheric physics, in space studies and other applications. In Brazil, with its continentally sized land area, there are only two operating lidar systems; the first is devoted to stratospheric studies (Clemesha and Rodrigue 1971) and the second, an elastic backscatter lidar system, is devoted to tropospheric aerosol profiling for air pollution applications. This limited number of lidar systems is in contrast to the large networks now in operation over Europe and North America.

The lidar technique principle is based on the emission of a laser beam in the atmosphere and the detection of the backscattered laser light by the suspended atmospheric aerosols and its analysis, in real time, with high temporal (some seconds) and spatial (a few metres) resolution (Ferrare *et al.* 1991, Marenco *et al.* 1997). This method of studying the lower atmosphere relies on the fact that the aerosols are treated as passive tracers of the atmospheric dynamics, and thus, the lidar technique can provide information on the structure and parameters of the Planetary Boundary Layer (PBL) (Melfi *et al.* 1985, Crum *et al.* 1987, Papayannis and Balis 1998, Balis *et al.* 2000, Papayannis and Chourdakis 2002). Besides, the synergy of ancillary meteorological measurements and simultaneous investigations of the optical properties of the suspended aerosols (by Sun photometers or spectrophotometers) can provide additional information for reducing the lidar data retrieval errors (aerosol extinction and backscatter profiles). Especially, this synergy of measurements helps to minimize the uncertainties of the assumptions made, when inverting the lidar signals (Takamura *et al.* 1994, Marenco *et al.* 1997, Balis *et al.* 2000) using the input value of the extinction-to-backscatter ratio (lidar ratio), since it is well known that the lidar ratio has a wide range of values, which depend on the

Downloaded by [USP University of Sao Paulo] at 08:21 30 April 2013

relative humidity (RH) and on the origin of the air masses sampled (Ackermann 1998, Anderson *et al.* 2000).

The purpose of this paper is to present the first ground-based lidar measurements of suspended aerosol particles in the PBL and the adjacent free troposphere (1.5–5 km height) performed over the city of São Paulo, Brazil (23°33′ S, 46°44′ W) during the second half of the Brazilian dry season. Previous airborne measurements of suspended aerosol particles and ozone have been carried out by the National Aeronautics and Space Administration (NASA) lidar group during the GTE/ABLE 2B campaign over the Amazon area during the wet season (Browell *et al.* 1990).

Aerosol optical thickness measurements (AOT) were also performed with a commercial CIMEL Sun photometer, in order to help the interpretation of the lidar measurements, taken under 'cloud-free' conditions during the last period of the wintertime or dry season, September and October months, since the distinction amongst the seasons in the São Paulo region is not very pronounced. Some selected days were taken as case studies and for these days air mass backward trajectories were calculated using the University of São Paulo Trajectory Model (USPTM) (Freitas *et al.* 1996) in order to attain the height and origin of the aerosol load into the metropolitan area of São Paulo (MASP). The instrument locations in the São Paulo district area are depicted in figure 1. The daily CIMEL and lidar data were acquired in a different time frame, mostly due to operational issues. In §2 of this paper a brief overview of the experimental set-up of the lidar system and the CIMEL photometer will be given. In §3 a brief presentation of the USPTM model will be presented. In §4 the lidar inversion technique and data analysis will be presented. In §5 three case studies of aerosol lidar measurements will be analysed and discussed. Finally, §6 presents a discussion and our concluding remarks.

Downloaded by [USP University of Sao Paulo] at 08:21 30 April 2013

2. Experimental set-up

2.1 *Lidar system*

A ground-based elastic backscatter lidar system has been recently developed in the Laboratory of Environmental Laser Applications at the Centre for Laser and

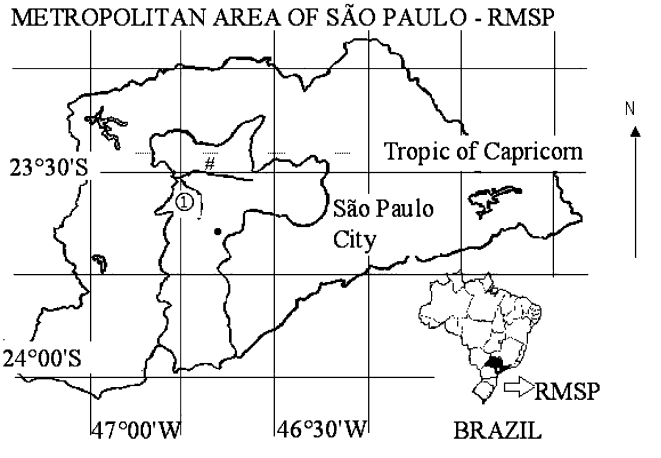

Figure 1. São Paulo Metropolitan Region (MASP=RMSP) map with the sampling locations indicated: (1), São Paulo University Campus (USP), site of the lidar and CIMEL; •, meteorological station.

Applications (CLA) at the Instituto de Pesquisas Energéticas e Nucleares (IPEN) (figure 2). The lidar system is a single-wavelength backscatter system pointing vertically to the zenith and operating in the coaxial mode.

The light source is based on a commercial Nd:YAG laser (Brilliant by Quantel SA) operating at the second harmonic frequency (SHF), namely at 532 nm, with a fixed repetition rate of 20 Hz. The average emitted power can be selected up to values as high as 3.3 W. The emitted laser pulses have a divergence of less than 0.5 mrad. A 30 cm diameter telescope (focal length $f=1.3$ m) is used to collect the backscattered laser light. The telescope's field of view (FOV) is variable (0.5–5 mrad) by using a small diaphragm. The lidar is currently used with a fixed FOV of the order of 1 mrad, which according to geometrical calculations (Chourdakis *et al.* 2002) permits a full overlap between the telescope FOV and the laser beam at heights higher than 300 m above the lidar system. This FOV value, in accordance with the detection electronics, permits the probing of the atmosphere up to the free troposphere (5–6 km asl). To take into account the non-full overlap below 300 m, an overlap factor correction could be employed (Chourdakis *et al.* 2002). Among the experimental methods proposed to determine the lidar overlap factor, two techniques have to be mentioned: one method proposed by Sasano *et al.* (1979) and by Pavlow *et al.* (2004), in which multi-angle lidar profiles are employed, and one method based on the Raman scattering due to the atmospheric nitrogen, as recently shown by Wandinger and Ansmann (2002). However, such Raman channel is not currently available, and is foreseen for the near future upgrade of our system. This will enable us to determine the aerosol extinction and the aerosol backscatter coefficients independently at 355 nm (Ansmann *et al.* 1990).

The backscattered laser radiation is then sent to a S-20 photomultiplier tube (PMT) coupled to a narrow band (1 nm FWHM) interference filter, to ensure the reduction of the solar background during daytime operation and to improve the signal-to-noise ratio (SNR) at altitudes greater than 3 km. The PMT output signal is recorded by a 1 GHz digitizing oscilloscope—Tektronix 580 TDS—presenting a 10 bit analogue-to-digital conversion (ADC) resolution. Data are

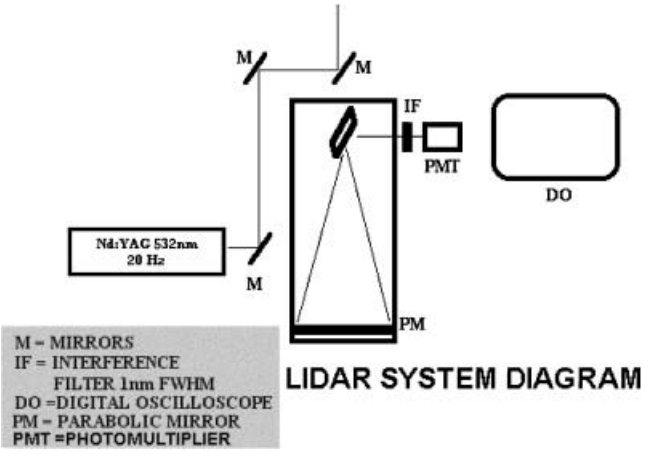

Figure 2. Single-wavelength elastic backscatter lidar system experimental set-up.

Downloaded by [USP University of Sao Paulo] at 08:21 30 April 2013

averaged between 2–5 min and then summed up over a period of about 1 h, with a typical spatial resolution of 15 m, which corresponds to a 100 ns temporal resolution.

2.2 *Sun-tracking photometer*

The CIMEL 318A spectral radiometer is a solar-powered weather-hardy robotically pointed Sun and sky instrument. This instrument is installed on the roof of the Physics Department at the University of São Paulo. The CIMEL photometer performs measurements of the AOT at several wavelengths in the visible and the near-infrared spectral region to enable the assessment also of the Ångström coefficient (Holben *et al.* 2001). The principle of operation of this system is to acquire aureole and sky radiances observations using a great number of scattering angles from the Sun, through a constant aerosol profile to retrieve the aerosol size distribution, the phase function and the AOT. For the relevant study, the channels used are centred at 340, 440, 500, 670, 870, 940 and 1020 nm, with a 1.2° full angle FOV. The measurements are taken pointed directly to the Sun (four sequences) or to the sky (five sequences) in nine different pre-programmed sequences (Holben *et al.* 1998). Three of them are dedicated to retrieve the AOTs, while the other six are taken to obtain the calibration parameters, the sky radiance, the aerosol particle size distribution, the refractive index (both real and imaginary components), the phase function, the total column abundance and the perceptible water content (Dubovik and King 2000). The standard measurements are taken in 15 min interval, in order to allow cloud contamination checking. These measurements are taken in the whole spectral interval, and their number depends on the daytime duration. The instrument precision and accuracy follow the standard Langley plot method within the standard employed by the AERONET network (Holben *et al.* 1998). The CIMEL Sun photometer is calibrated periodically by a remote computer or locally under the supervision of the AERONET network. The calibration methodology assures a coefficient error between 1% and 3%; nonetheless, various instrumental, calibration, atmospheric, and methodological factors influence the precision and accuracy of the derived optical thickness and effectively the total uncertainty in the AOT is about 10% (Dubovik *et al.* 2000).

3. Modelling

The air-mass backward trajectory calculations apply a three-dimensional (3D) kinematic trajectory model which was developed at the University of São Paulo (Freitas *et al.* 2000). The air mass trajectories (called kinematic trajectories) are obtained using the three components of the wind field, which is numerically generated by the Regional Atmospheric Modeling System approach (RAMS) as shown by Pielke *et al.* (1992) and by Liston and Pielke (2001). The air parcel trajectory output is generated every 3 min, thus providing the latitude, longitude and altitude coordinates. In this paper we show the trajectory locations every 6 h using a colour-coded scale. The model time period extends to about one week, while the corresponding spatial resolution is about 60 km (Freitas *et al.* 2000). In this paper we calculated 96-h (four days) back-trajectories of air masses ending over the city of São Paulo, in order to have a more realistic input about the origin of the air masses ending over our lidar site and to locate the aerosols sources near the São Paulo region.

Downloaded by [USP University of Sao Paulo] at 08:21 30 April 2013

4. Data analysis and methodology

4.1 *Lidar inversion algorithm*

In the present stage, the retrieval of the aerosol optical properties is based on the measurements of the aerosol backscatter coefficient (β_{aer}) at 532 nm, up to an altitude of 5–6 km asl. The determination of the vertical profile of the aerosol backscatter coefficient relies on the lidar inversion technique following the Klett's algorithm, as proposed by Klett (1985) and Fernald (1984), where no multiple scattering correction is applied, under the assumption of elastic scattering by spherical aerosols. It is well known that multiple scattering occurs mostly under low-visibility conditions (presence of water droplets, ice crystals, fog, haze, etc.). As stated by Measures (1992) depolarization ratio values in excess of about 0.02 can arise from spherical particles (water droplets) in the event of multiple scattering. If the scattering particle is non-spherical (such as ice crystals, dust and biomass burning particles) the depolarization ratio increases (Measures 1992) and typically ranges between 0.2 and 0.5 (Tataro *et al.* 2004). Depolarization studies can thus provide some insight into the distribution of ice and water in clouds and also can help to discriminate between spherical and non-spherical atmospheric aerosols.

In this paper we did not consider multiple-scattering effects, since no low-visibility conditions were taken into account. The valuable information given by depolarization of the incident linearly polarized laser beam is not available in the actual version of our lidar system. However, a depolarization channel at 532 nm is foreseen in the next phase of upgrade of our aerosol lidar system; therefore, we will have the possibility to distinguish between spherical (such as dust or biomass aerosols) and non-spherical (such as ice crystals) particles under high-visibility conditions (no multiple-scattering effects).

One has, however, to bear in mind that this inversion technique is an ill-posed problem in the mathematical sense, leading to errors as large as 30% when applied (Papayannis and Chourdakis 2002). In general, the inversion of the lidar profile is based on the solution of the basic lidar equation (equation (1)), taking into account the atmospheric solar background radiation correction (Measures 1992, Papayannis and Chourdakis 2002):

$$P(\lambda, R) = P_L\left(\frac{c\tau}{2}\right)\beta(\lambda, R)A_o\xi(\lambda)\zeta(R)R^{-2}\exp\left[-2\int_0^R \alpha(\lambda, r)\mathrm{d}r\right] \quad (1)$$

where, $P(\lambda,R)$ is the lidar signal received from a distance R at the wavelength λ, P_L is the emitted laser power, A_0 is the telescope receiving area, $\xi(\lambda)$ is the receiver's spectral transmission factor, $\beta(\lambda,R)$ is the atmospheric volume backscatter coefficient, $\zeta(R)$ is the overlap factor between the FOV of the telescope and the laser beam, $\alpha(\lambda, R)$ is the extinction coefficient, c is the light speed and τ is the laser pulse length.

In equation (1), the α and β coefficients can be separated into two sets, one for the molecular scattering component and the other for the particle scattering component. Besides, in the Klett inversion technique, there is a reference altitude, $Z_{ref,}$ which is used as an upper limit, and has to be an aerosol-free region. Therefore, in this region and above it, the lidar signal shows a decay, which follows the molecular contribution only. This is regularly checked using the technique proposed by Chourdakis *et al.* (2002), in which the lidar signal perfectly fits to the signal corresponding to the molecular atmosphere in an aerosol-free region, and thus

Downloaded by [USP University of Sao Paulo] at 08:21 30 April 2013

always assures the perfect alignment of the lidar system. In our case the Z_{ref} value was taken in the 7–9 km region, using the technique proposed by Chourdakis *et al.* (2002).

To retrieve the aerosol backscatter coefficient we applied the Klett's inversion technique assuming a 'guessed' altitude-constant extinction-to-backscatter ratio (LR) in the lower troposphere, given by:

$$\beta_p / \alpha_p = C = 1/\text{LR} \tag{2}$$

However, it is known that the LR depends on several parameters, such as the aerosol refractive index, the shape and size distribution of the aerosol particles. Besides, there is a strong dependence of LR on the temperature and humidity profiles in the atmosphere, that might cause variations on the optical parameters of the aerosols (Haenel 1976), and of course on the presence of turbulence in the atmospheric volume being probed by the lidar beam (Stull 1991).

To derive the appropriate 'correct' values of the vertical profile of aerosol backscatter coefficient in the lower troposphere we used an iterative inversion approach (by 'tuning' the LR values) based on the inter-comparison of the AOT values derived by lidar and CIMEL data, assuming the absence of stratospheric aerosols and that the PBL is homogeneously mixed between ground and 300 m height, where the lidar overlap factor is close to 1. Once the 'correct' values of the vertical profile of aerosol backscatter coefficient were derived (when the difference of the AOTs derived by CIMEL and lidar was less than 10%) we reapplied the Klett method, using the appropriate LR values, to retrieve the final values of the vertical profiles of the backscatter and extinction coefficient at 532 nm.

The accuracy of the lidar measurements is such that up to 4 km the statistical error is of the order of 5–10%, since the SNR of our lidar signals remains higher than 3.5 (Marenco *et al.* 1997). As discussed before, the systematic error on the retrieval of the backscatter coefficient β_p can be as high as 30%, depending mainly on the mean value of C used (Balis *et al.* 2000). This systematic error can be minimized using an iterative algorithm by direct measurements of the AOT from co-located CIMEL measurements, using the relation:

$$\text{AOT} = \sum_{0}^{R_{\text{ref}}} \alpha(r) \Delta r \tag{3}$$

where Δr is the vertical sampling resolution of the lidar measurements, normally taken as 0.015 km.

4.2 *CIMEL inversion algorithm*

The inversion of the solar radiances measured by the CIMEL Sun photometer to retrieve the aerosol optical thickness values is based on the Beer–Lambert equation, assuming that the contribution of multiple scattering within the small FOV of the Sun photometer is negligible:

$$I_\lambda = I_\lambda^0 \exp\left(- \frac{\tau_\lambda}{\mu_S} \right) \tag{4}$$

where $I^0{}_\lambda$ and I_λ are the solar irradiances at ground level and at the top of

Downloaded by [USP University of Sao Paulo] at 08:21 30 April 2013

the atmosphere, respectively, and μ_S is the cosine of the solar zenith angle. τ_λ is the total atmospheric optical thickness from the Rayleigh and aerosol contributions, as well the ozone and water vapour absorption at 670 nm and 870 nm, respectively, bearing in mind that the ozone contribution is also subtracted from the total optical depth. The aerosol optical thickness at 532 nm was determined by the relation:

$$\frac{\tau_{532}^{\text{aer}}}{\tau_{500}^{\text{aer}}} = \left(\frac{532}{500}\right)^{-\alpha} \tag{5}$$

where the Ångström exponent (Ångström 1964) α was derived from the measured optical thickness in the blue and red channels (440 nm and 670 nm):

$$\alpha = -\frac{\log\left(\tau_{440}^{\text{aer}}/\tau_{670}^{\text{aer}}\right)}{\log(440/670)} \tag{6}$$

The Ångström exponent is also an indirect mean to retrieve the particle size distribution (Junge 1963) and its possible composition (Deepak and Gerber 1983, D'Almeida *et al*. 1991). Concerning the uncertainty, the major source of error would be in the calibration procedure, which is proportional to the associated uncertainty of the AOT at a given wavelength (Hamonou *et al.* 1999).

5. Data analysis

In this paper we will present three selected cases for the year 2001: 19 and 24 September and 3 October. For these three cases we will focus on the following issues: the meteorological conditions during the measurements, the optical thickness measured by the lidar and the Sun photometer, the PBL structure and the air mass back trajectory analysis at various altitudes. For the sake of comparison and categorization, three distinct criteria are here applied in order to have a 'guess' of the lidar ratio:

(1) the first criterion (LR_1), where the lidar's AOT is given by inversion analysis using the LR extracted from the Sun photometer data;
(2) The second criterion (LR_2), where the CIMEL-retrieved AOT is applied to tune the LR, in such a way that a LR is used in the lidar inversion analysis to obtain an AOT about 10% of that retrieved by the CIMEL. In this instance, this value is a rough estimation of the contribution not taken into account by the lidar system due the overlap factor (equals the unity above 300 m); and
(3) the last criterion (LR_3), where the CIMEL-retrieved AOT is also applied to tune the LR, in such a way that a LR is used in the inversion analysis to obtain the same AOT in both lidar and CIMEL.

It is interesting to note, as will be explained in detail in the next paragraphs, that the AOT derived by the lidar measurements is generally lower than that derived by the CIMEL instrument. This is due of course to the fact that the lidar system is not able to probe the lower part (0–300 m) of the atmosphere (Chourdakis *et al*. 2002), where an important fraction of aerosol particles is present. Therefore, during days of high air pollution loads in the PBL the difference between the lidar- and the CIMEL-derived AOTs becomes significant.

The ideas mentioned in the three sections above can be summarized in two tables. The first table (table 1) shows the synoptic meteorological conditions of each day

Downloaded by [USP University of Sao Paulo] at 08:21 30 April 2013

Table 1. Meteorological conditions during measurements.

Day	Daily maximum and minimum temperature (°C) at ground level	Daily maximum and minimum relative humidity (%) at ground level	Temperature during lidar measurements (° C)	Relative humidity during lidar measurements (%)	Lidar derived PBL height (m)
19 September 2001	10.4–23.0	33–95	22.0	37–40	750
24 September 2001	15.0–27.7	48–97	26.0	44–50	600
3 October 2001	14.0–25.2	41–88	23.0	49–54	550

Downloaded by [USP University of Sao Paulo] at 08:21 30 April 2013

and gives also the structure of the atmosphere, namely the PBL height, as derived by the lidar measurements, using the approach proposed by Menut *et al.* (1999). Table 2 gives the optical properties of the atmosphere and the AOTs as derived from the CIMEL and lidar measurements, as well the lidar ratio applied to get the lidar-derived optical thickness. One will observe that there are some large discrepancies between the CIMEL LR and the two other values given in table 2; these discrepancies might be related to the impossibility of having the same time frame for the data acquisition, besides the figures obtained by the CIMEL oscillate more than 20% in value within a few minutes of data acquisition, which might relate to the high sensitivity of the CIMEL for the parameters used to obtain the LR, namely the Phase function and Single Scattering Albedo, used to retrieve the LRs from the Sun photometer data (Welton *et al.* 2002).

5.1 *19 September 2001*

The day of 19 September was characterized by a ground temperature ranging throughout the day from 10.4–23°C, accompanied by a change in the RH from 33% to 95%. The lidar profiles (aerosol backscatter coefficient) taken between 14:00 and 15:00 UTC (figure 3) indicate the presence of a first aerosol layer up to 750 m.

Table 2. Atmospheric optical thickness (AOT) as derived by CIMEL and lidar data.

Day	LR_1	LR_2	LR_3	AOT_1	AOT_2	AOT_3	Ångström exponent
19 September	73 ± 7	45 ± 6	43 ± 6	0.15 ± 0.02	0.12 ± 0.02	0.25 ± 0.03	1.9 ± 0.3
24 September	39 ± 4	41 ± 5	45 ± 6	0.35 ± 0.03	0.31 ± 0.04	0.29 ± 0.04	1.5 ± 0.2
3 October	N/A	16 ± 2	19 ± 3	N/A	0.05 ± 0.01	0.04 ± 0.01	1.6 ± 0.2
3 October	N/A	14 ± 2	15 ± 3	N/A	0.07 ± 0.01	0.06 ± 0.02	1.6 ± 0.2

Day: Days of the year 2001 the measurements were performed.
LR_1: Lidar ratio retrieved from CIMEL.
LR_2: Lidar ratio used by lidar with the 10% approach.
LR_3: Lidar ratio applied to obtain a matching between the AOTs provided by CIMEL and lidar.
AOT_1: AOT provided by the CIMEL.
AOT_2: AOT provided by the lidar.
AOT_3: AOT provided by the lidar using the LR_1.
On 3 October two measurements were carried out: one in the morning (local time) and the other in middle afternoon. Also the CIMEL data needed for the LR estimation (single scattering albedo and phase functions) were not available on this day.

During this period of measurements there are some changes in these lower structures, which could originate from nearby local aerosol sources, as the mixing layer did not evolve to higher heights and thus a 'practically' aerosol-free atmosphere is found above 1500–2000 m height. In this context the aerosol load observed inside the PBL sources is due mainly to local urban activities, like car traffic, industrial emissions and other urban sources.

As the altitude increases one can observe a discrete residual layer up to 2.5 km, which is probably the entrainment zone with an upper limit around 3 km. Above this altitude, a free and cleaner atmosphere is reached. The 3D 96-h air mass back-trajectory analysis for air parcels ending over our site at 14:00 UTC at two height levels (1200 and 2500 m asl) (figure 4(*a*) and (*b*), respectively) shows the origin of these incoming air masses being the marine boundary layer and neighbouring suburban regions. It is interesting to note that the air masses arriving at 1200 m height originated from an altitude of about 300 m asl over the ocean. Therefore, from these plots one could propose that there is a mixing of maritime and continental aerosols, along with those generated inside the MASP itself.

The AOT values obtained at 532 nm on 19 September 2001 were 0.15 ± 0.02 and 0.25 ± 0.03 for the CIMEL and lidar systems, respectively, taking into account that the LR input value, for the Klett inversion technique, was taken equal to 45 sr. Similar values of the LR at 532 nm were recently reported by Mueller *et al.* (2001) and by Wandinger *et al.* (2002) for urban air polluted air masses during the INDOEX experiment.

5.2 *24 September 2001*

The day of 24 September was characterized by a ground temperature ranging throughout the day from 15.0–27.7°C, accompanied by a change in the RH from

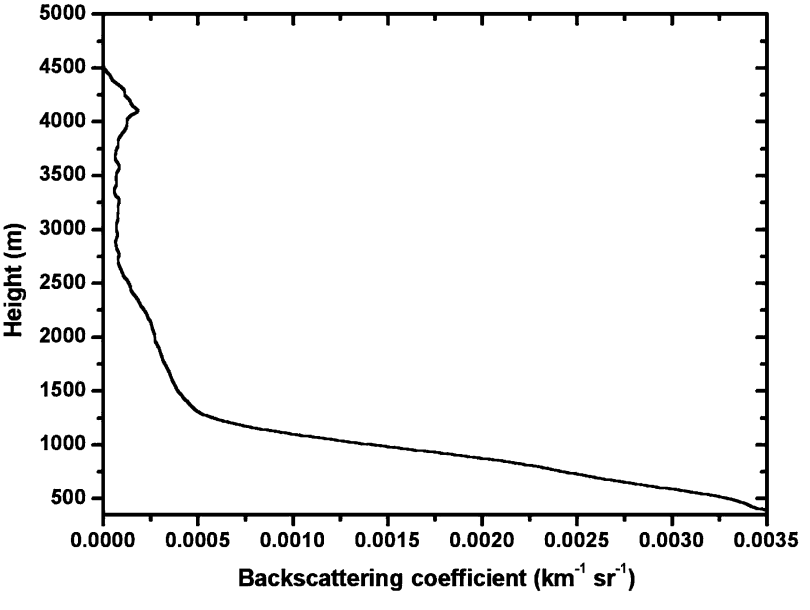

Figure 3. Aerosol backscatter coefficient profiles taken from 14:00 to 15:00 UTC on 19 September 2001.

Downloaded by [USP University of Sao Paulo] at 08:21 30 April 2013

Downloaded by [USP University of Sao Paulo] at 08:21 30 April 2013

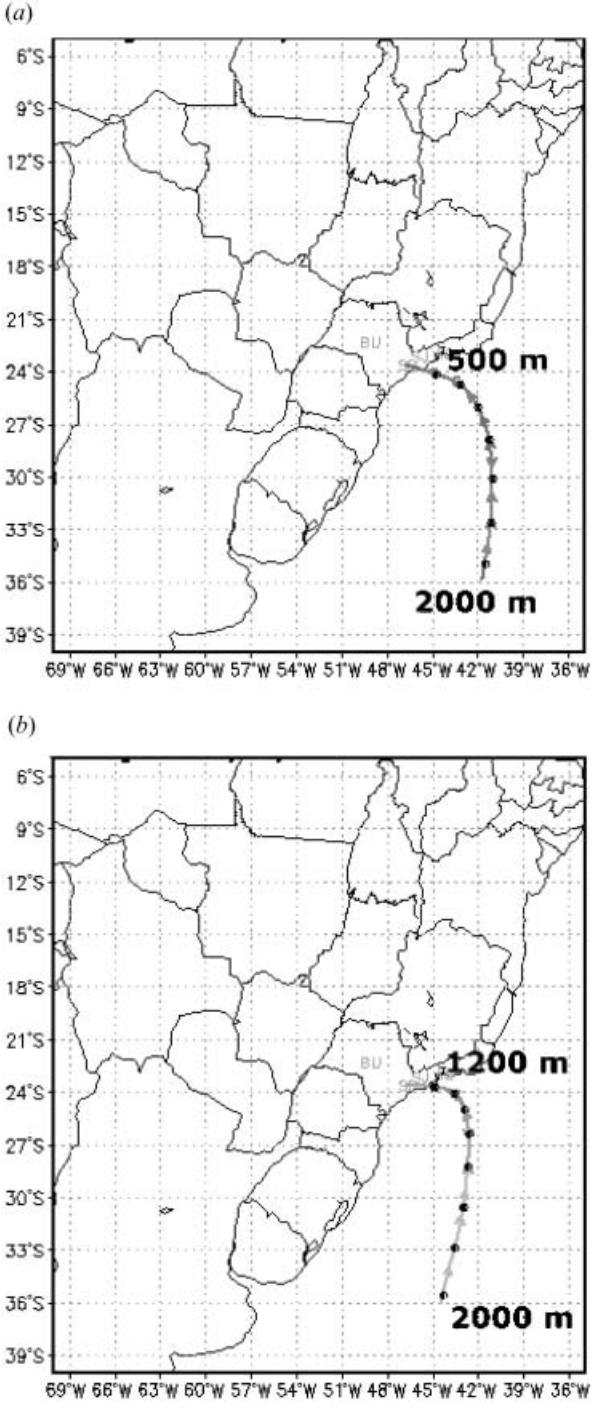

Figure 4. Three-dimensional air mass backward (96 h iteration) trajectories on 19 September 2001, 14:00 UTC, arriving at different altitudes: (*a*) 1200 m, and (*b*) 2500 m.

48% to 95%. The previous days, 21 and 22, were cloudy with high RH values (85%) at ground level and a stable ground temperature of about 17°C. On 23 September the ground temperature rose to 22°C.

The aerosol backscatter profiles taken between 13:00 and 14:00 GMT, on 24 September, are shown in figure 5. In this profile intense aerosol layers are present around 1500–2000 m and above 2500 m. These aerosol layers as well as the very thick layer observed between 2500 and 6000 m, are probably indicative of the presence of long-range transported particles in the free troposphere originating from remote areas. The mean AOT derived values from the CIMEL data at 532 nm on 24 September 2001 were quite high, of the order of 0.35. If we include again the assumed well-mixed first 300 m and match the lidar and CIMEL AOT values to within 10%, we find a mean LR of the order of 41 sr.

As we did not take samples of the aerosols along the laser beam propagation into the atmosphere, we cannot actually comment on the chemical type of such aerosols. Instead, we can only speculate on their apparent size and their source region. The Ångström exponent values obtained for that day (0.6 ± 0.20) indicate probably the presence of rather small aerosol particles, probably like the carbonaceous particles or even smoke-aged aerosols diluted over the urban area of São Paulo (Eck *et al.* 1999).

The origin of such intense aerosol layers can be found if one looks at the three-dimensional 96-h air mass backward trajectories (figure 6(*a*) to (*c*) ending at 1000, 2000 and 4500 m above ground level at 12:00 UTC. The low altitude content of aerosols (around at 1000 m) is probably due to the local industrial sites in the city and the heavy car traffic. In addition, the low air mass dispersion conditions of the previous days should be added to the total aerosol load present at the time of measurements. Another important aspect to focus on is the presence of intense aerosol layers seen at altitudes higher than 2 km height. As one can see from

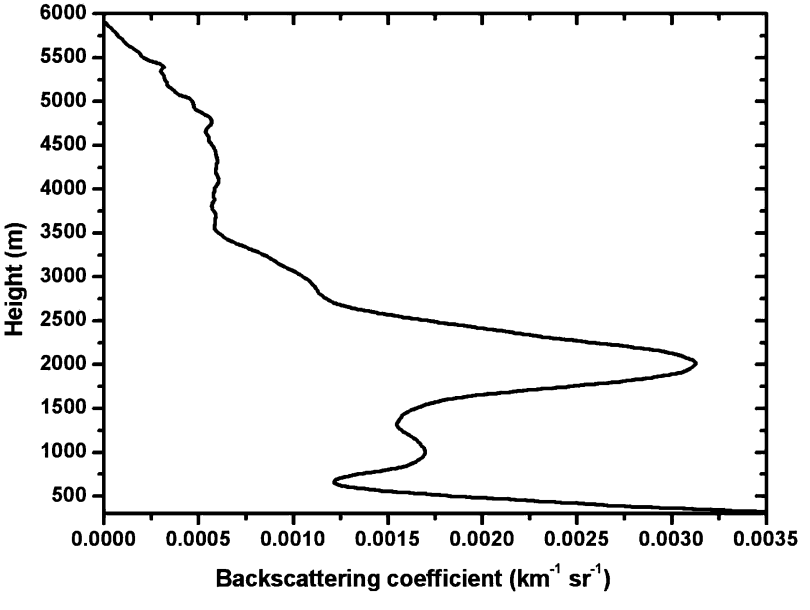

Figure 5. Aerosol backscatter coefficient profiles taken between 13:00 to 14:00 UTC on 24 September 2001.

Downloaded by [USP University of Sao Paulo] at 08:21 30 April 2013

Downloaded by [USP University of Sao Paulo] at 08:21 30 April 2013

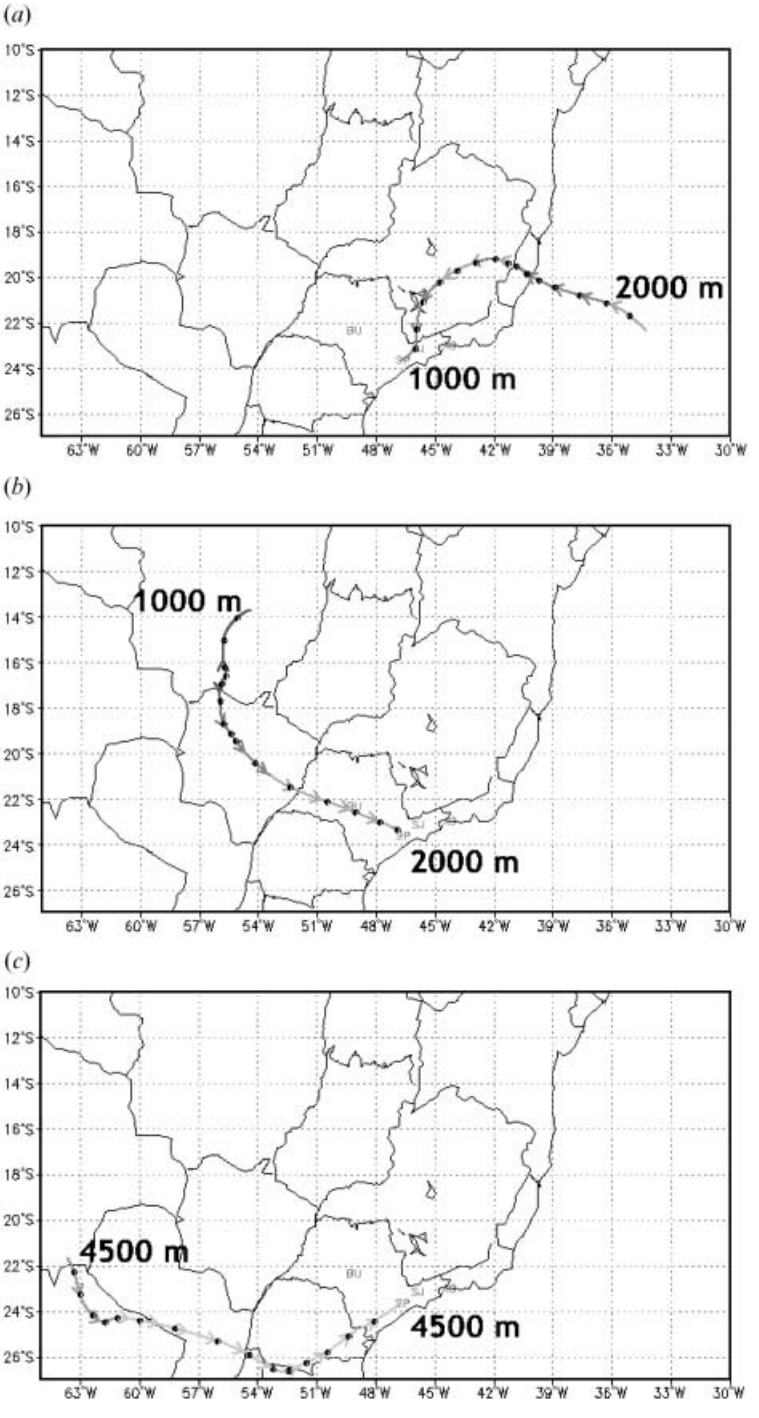

Figure 6. Three-dimensional air mass backward (96 h iteration) trajectories, on 24 September 2001, 12:00 UTC, arriving at different altitudes: (*a*) 1000 m, (*b*) 2000 m, and (*c*) 4500 m.

figure 6(*b*) and (*c*), the air mass back-trajectory analysis shows that at 2000 m and 4500 m, respectively, the aerosol particles are coming from the western part, that is, the country side of the state, where biomass burning is very common during that season.

5.3 *3 October 2001*

3 October was a very clear day with a few scattered high clouds, following a series of rainy days responsible for washing out the pollution accumulated until then. The ground temperature ranged throughout the day from 14.0–25.2°C, accompanied by a change in the RH from 41% to 88%.

The lidar profiles (figure 7) show that this day was favourable to atmospheric convection, with a less dense but thicker (than the one shown in case II) aerosol layer, starting at about 600 m height and ending at about 4.0 km. As this day was preceded by rainy days, the stronger sources of aerosols were mainly local. The changes in the aerosol backscatter profiles were significant during this short period of measurements, even though it was a very 'clear' day with favourable dispersion conditions, under windy meteorological conditions. In figure 7 one can also observe the presence of an intense aerosol layer around 1.2 km height, which again would probably correspond to the top of the PBL.

If we consider the 3D 96-h air mass backward trajectory analysis for air masses ending at 18:00 UTC over our site (figure 8(*a*) to (*c*)) we realize that the air masses sampled originated from the western part of the continent, in the height region between 1500 and 3500 m. Advection of air masses containing biomass burning aerosols could be speculated to be the reason for the aerosol layers observed that day.

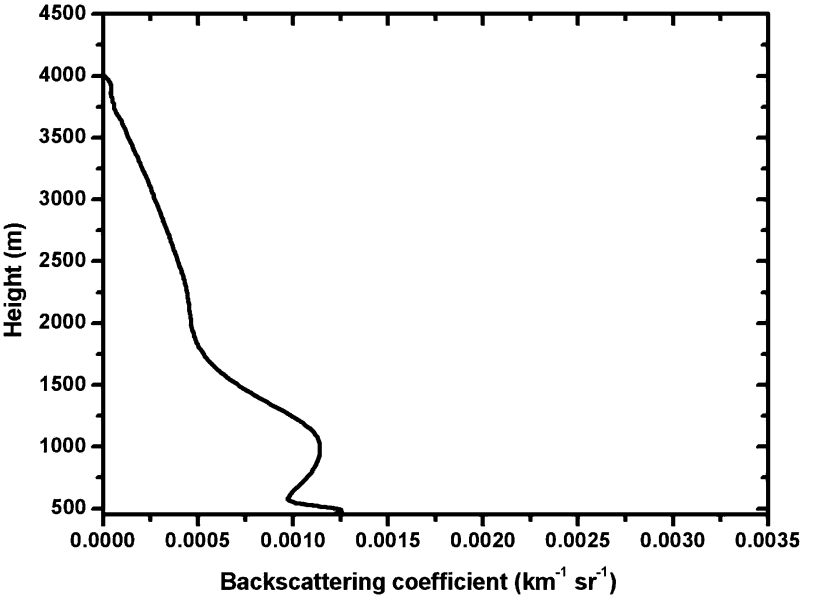

Figure 7. Aerosol backscatter coefficient profiles taken from 18:00 to 18:30 UTC on 3 October 2001.

Downloaded by [USP University of Sao Paulo] at 08:21 30 April 2013

Downloaded by [USP University of Sao Paulo] at 08:21 30 April 2013

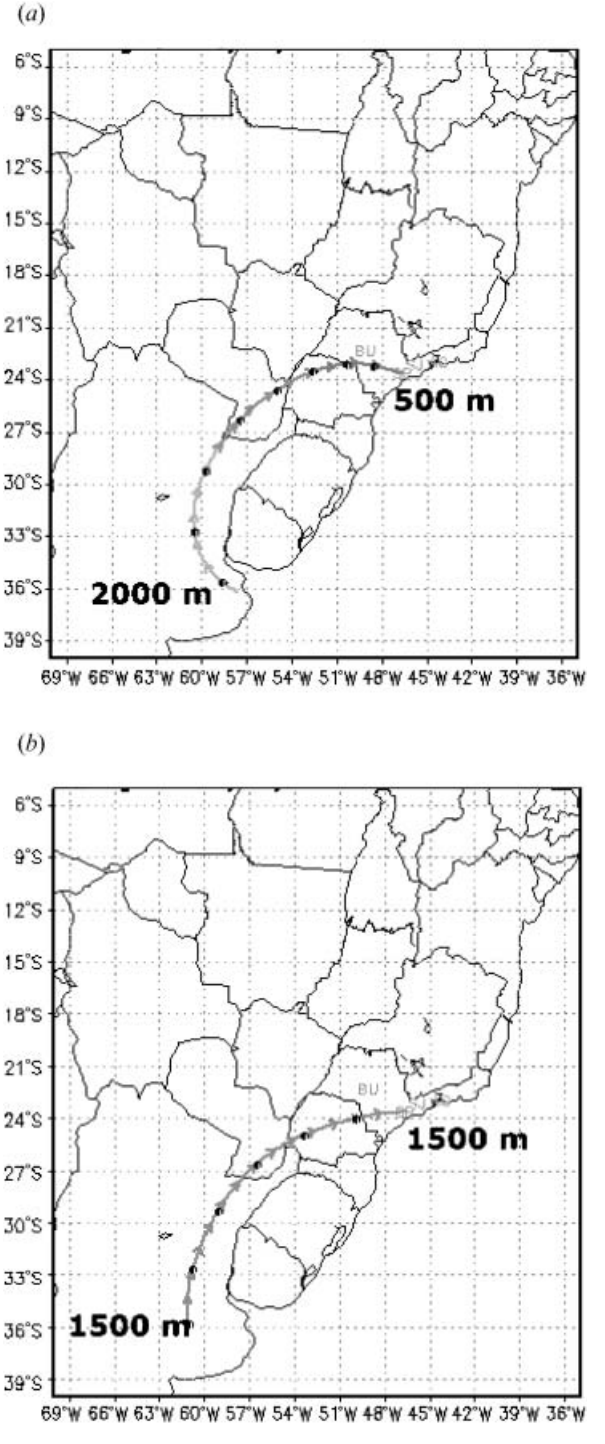

Figure 8. Three-dimensional air mass backward (96 h iteration) trajectories, on 3 October 2001, 18:00 UTC, arriving at different altitudes: (*a*) 500 m, (*b*) 1500 m, and (*c*) 3500 m.

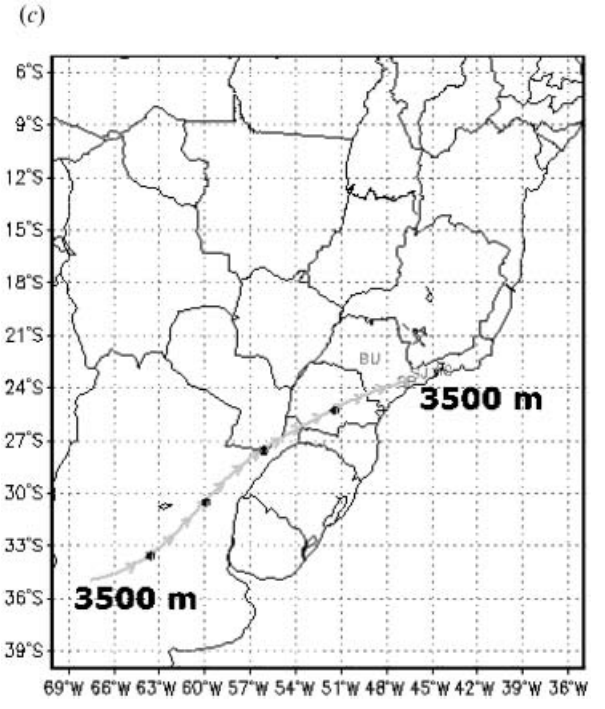

Figure 8. (*Continued*).

The average optical thickness retrieved by the CIMEL Sun photometer was around 0.08 ± 0.03, and was taken around 18:00 UTC, with a corresponding Ångström exponent of 2.0 ± 0.5, which corresponds to finer particles than the other case studies. The lidar profiles shown in figure 7 were taken between 18:00 and 19:00 UTC, thus the lidar derived average AOT is 0.07 ± 0.02, and was calculated from 0.4 to 5.0 km. The lidar derived AOT was 13% smaller than the AOT given by the Sun photometer. This again can be explained by the fact that the full overlap of the lidar system occurs at altitudes higher than 300 m.

6. Discussion and conclusions

The results from the first lidar measurements performed during the second half of the so-called *dry season*, September and October 2001 in São Paulo, Brazil, showed a significant variability of the AOT at 532 nm in the lower troposphere (0.5–5 km). The maximum value of the AOT retrieved by CIMEL was 0.44 ± 0.05, and was valid for clear-sky conditions on 24 September 2001. This AOT variability was also confirmed from co-located aerosol lidar measurements. The first tropospheric aerosol measurements performed over the city of São Paulo during the dry season showed that the aerosol load is maximized in the 1–3 km height and represents about 20–25% of the suspended aerosol particles in the troposphere. The variability of the suspended aerosols in this layer increases when long-range transport mechanisms are involved, transferring dust from industrial or biomass burning regions over our measuring site. This is validated when 4-day 3D air mass backward trajectory analysis is performed. The synergy of the lidar and Sun photometer measurements indicated that the aerosols over the measuring site were most probably composed by carbonaceous particles and anthropogenic or biogenic sulphate ones.

Downloaded by [USP University of Sao Paulo] at 08:21 30 April 2013

The absolute value changes in the AOTs reflect the fact that the days the measurements were taken presented different meteorological and therefore pollution dispersion conditions. Namely, the day 24 September, which was the most heavily polluted, was characterized by the high optical thickness values given by the CIMEL and the lidar systems (of the order of $0.30\,km^{-1}$), while days 19 September and 3 October were less polluted showing smaller values of OTs (of the order of $0.15\,km^{-1}$ and $0.05\,km^{-1}$, respectively).

The CIMEL data for the three selected days were also used to derive the Ångström exponent over the city of São Paulo, from which the corresponding mean lidar ratio values were derived using the available data in the literature as given by D'Almeida *et al.* (1991). The mean lidar ratio over our urban region during the dry season is of the order of 36–45 sr. Additionally, when correlating the value of the lidar ratio and the Ångström exponent, one realizes, following the procedure described by Anderson *et al.* (2000), that the aerosol load is on the accumulation mode instead of the coarse mode; this is also corroborated by Ångström exponent values themselves as exposed in the literature by D'Almeida *et al.* (1991). Attention has to be given to the fact that under high aerosol optical depth conditions the first 300–400 m, which were not included in the lidar measurements, may contain an important fraction of the tropospheric aerosol load. This could be a potential reason why there were some discrepancies among the LR_2 and LR_3 values derived.

The lidar system is now being 'upgraded' to a Raman lidar and 532nm-polarization system, in order to provide profiles of the aerosol depolarization at 532 nm and the aerosol extinction at 355 nm (Müller *et al.* 1998). For such a task a third-harmonic generator module has been added to the laser head allowing the possibility of emitting a laser beam at 355 nm as well, and detecting the 355 nm signal together with the Nitrogen Raman signal at 387 nm. For adding this module the detection system also has been remodelled with the appropriate optics as well.

The polarization channel, as we have named it, in the system was made with an addition of a Glan separator giving the possibility of analysing the depolarization of the original laser incident beam (parallel polarization) in the atmosphere, we expect after developing the proper software for studying the data we might be able to get size and morphology distribution of the particles in the atmosphere.

With such improvement we expect then a better inter-comparison with ground-based instrumentation and other airborne instruments such as balloons and/or satellites.

Downloaded by [USP University of Sao Paulo] at 08:21 30 April 2013

Acknowledgments

The authors are grateful for the financial support given by the federal agency Conselho Nacional de Desenvolvimento Científico e Tecnológico (CNPq) and by the State of São Paulo agency Fundação de Amparo à Pesquisa (FAPESP) under contract numbers 620009/98-5 and 98/14891-2, respectively. They would like also to thank the anonymous reviewers for their helpful comments and remarks.

References

Ackermann, J., 1998, The extinction-to-backscatter ratio of tropospheric aerosol: a numerical study. *Journal of Atmospheric and Oceanic Technology*, **15**, pp. 1043–1050.

Alonso, C.D., Martins, M.H.R.B., Romano, J. and Godinho, R., 1997, São Paulo aerosol characterization study. *Journal of Air and Waste Management Association*, **47**, pp. 1297–1300.

ANDERSON, T.L., MASONIS, S.J., COVERT, D.V., CHARLSON, R.J. and ROOD, M.J., 2000, In situ measurement of the aerosol extinction-to-backscatter ratio at a polluted continental site. *Journal of Geophysical Research*, **105**, pp. 26 907–26 915.

ÅNGSTRÖM, A., 1964, The parameters of atmospheric turbidity. *Tellus*, **16**, pp. 64–75.

ANSMANN, A., WANDINGER, U., RIEBESEL, M., WEITKAMP, C. and MICHELIS, W., 1990, Independent measurements of extinction and backscatter profiles in cirrus clouds by using a combined Raman elastic backscatter lidar. *Applied Optics*, **31**, pp. 7113–7131.

BALIS, D., PAPAYANNIS, A., GALANI, E., MARENCO, F., SANTACESARIA, V., HAMONOU, E., CHAZETTE, P., ZIOMAS, I. and ZEREFOS, C., 2000, Tropospheric LIDAR aerosol measurements and sun photometric observations at Thessaloniki, Greece. *Atmospheric Environment*, **34**, pp. 925–932.

BISSONNETTE, L., ROY, G. and VALLÉ, G., 2002, *21st Lidar Remote Sensing in Atmospheric and Earth Sciences*, Part I and Part II, 8 July 2002 (Quebéc: Defence R&D Canada).

BOESENBERG, J., ANSMANN, A., BALDASANO, J., BOEKMANN, C., CALPINI, B., CHAIKOVSKY, A., FLAMANT, P., HAGARD, A., MITEV, V., PAPAYANNIS, A., PELON, J., RESENDES, D., SPINELLI, N., TRICKL, T., VAUGHAN, G., VISCONTI, G. and WIEGNER, M., 2001, EARLINET: a European Aerosol Lidar Network. In *Advances in Laser Remote Sensing*, A. Dabas, C. Loth and J. Pelon (Eds) (Vichy, France: Ecole Polytechnique, France), pp. 155–158.

BOESENBERG, J., MATTHIAS, V., AMODEO, A., AMOIRIDIS, V., ANSMANN, A., BALDASANO, J.M., BALIN, I., BÖCKMANN, C., BOSELLI, A., CARLSSON, G., CHAIKOVSKY, A., CHOURDAKIS, G., COMERÓN, A., DE TOMASI, F., EIXMANN, R., FREUDENTHALER, V., GIEHL, H., GRIGOROV, A., HAGARD, A., IARLORI, M., KIRSCHE, A., KOLAROV, G., KOMGUEM, L., KREIPL, S., KUMPF, W., LARCHEVÊQUE, G., LINNÉ, H., MATTHEY, R., MATTIS, I., MEKLER, A., MIRONOVA, I., MITEV, V., MONA, L., MÜLLER, D., MUSIC, S., NICKOVIC, S., PANDOLFI, M., PAPAYANNIS, A., PAPPALARDO, G., PELON, J., PÉREZ, C., PERRONE, R.M., PERSSON, R., RESENDES, D.P., RIZI, V., ROCADENBOSCH, R., RODRIGUES, J.A., SAUVAGE, L., SCHENEIDENBACH, L., SCHUMACHER, R., SHCHERBAKOV, V., SIMEONOV, V., SOBOLEWSKI, P., SPINELLI, N., STACHLEWSKA, I., STOYANOV, D., TRICKL, T., TSAKNAKIS, G., VAUGHAN, G., WANDINGER, U., WANG, X., WIEGNER, M., ZAVRATANIK, M. and ZEREFOS, C., 2003, EARLINET: a European Aerosol Research Lidar Network to establish an aerosol climatology. Final report, No. 348.

BROWELL, E.V., GREGORY, G., HARRIS, R. and KIRCHHOFF, V.J., 1990, Ozone and aerosol distribution over the Amazon basin during the wet season. *Journal of Geophysical Research*, **95**, pp. 16 887–16 901.

CHOURDAKIS, G., PAPAYANNIS, A. and PORTENEUVE, J., 2002, Analysis of the receiver response for a non-coaxial lidar system with fiber-optic output. *Applied Optics*, **41**, pp. 2715–2723.

CLEMESHA, B.R. and RODRIGUE, S.N., 1971, Stratospheric scattering profile at 23 degrees south. *Journal of Atmospheric and Terrestrial Physics*, **33**, pp. 1119–1125.

CRUM, T., STULL, R. and ELORANTA, E., 1987, Coincident lidar and aircraft observations of entrainment into thermal and mixed layers. *Journal of Climate and Applied Meteorology*, **26**, pp. 774–788.

D'ALMEIDA G.A., KOEPKE, P. and SHETTLE, E.P., 1991, *Atmospheric Aerosols, Global Climatology and Radiative Characteristics* (Hampton, VA: Deepak Publishers).

DEEPAK, A. and GERBER, H.E., 1983, Aerosols and their climate effects. Series Report 55, International Council of Scientific Unions and WMO, Switzerland.

DUBOVIK, O. and KING, M., 2000, A flexible inversion algorithm for retrieval of aerosol optical properties from sun and sky radiance measurements. *Journal of Geophysical Research*, **105**, pp. 20 673–20 696.

Downloaded by [USP University of Sao Paulo] at 08:21 30 April 2013

DUBOVIK, O., SMIRNOV, A., HOLBEN, B.N., KING, M.D., KAUFMAN, Y.J., ECK, T.F. and SLUTSKER, I., 2000, Accuracy assessments of aerosol optical properties retrieved from Aerosol Robotic Network (AERONET) Sun and sky radiance measurements. *Journal of Geophysical Research*, **105**, pp. 9791–9806.

ECK, T.F., HOLBEN, B.N., REID, J.S., DUBOVIK, O., SMIRNOV, A., O'NEILL, N.T., SLUTSKER, I. and KINNE, S., 1999, Wavelength dependence of the optical depth of biomass burning, urban, and desert dust aerosols. *Journal of Geophysical Research*, **104**, pp. 31333–31349.

FERNALD, G.F., 1984, Analysis of atmospheric lidar observations: some comments. *Applied Optics*, **23**, pp. 652–653.

FERRARE, R., SCHOLS, J. and ELORANTA, E., 1991, Lidar observations of banded convection during BLX83. *Journal of Applied Meteorology*, **30**, pp. 312–326.

FREITAS, S.R., DIAS, M.A.F.S., DIAS, P.L.S., LONGO, K.M., ARTAXO, P., ANDREAE, M.O. and FISCHER, H.S., 2000, A convective kinematic trajectory calculation for low resolution atmospheric models. *Journal of Geophysical Research*, **105**, pp. 375–386.

HAENEL, G., 1976, The properties of atmospheric aerosol particles in function of the relative humidity at thermodynamic equilibrium with the scattering moist air. *Advances in Geophysics*, **19**, pp. 73–188.

HAMONOU, E., CHAZETTE, P., BALIS, D., DULAC, F., SCHNEIDER, X., GALANI, E., ANCELLET, G. and PAPAYANNIS, A., 1999, Characterization of the vertical structure of Saharan dust export to the Mediterranean basin. *Journal of Geophysical Research*, **104**, pp. 22 257–22 270.

HOLBEN, B.N., ECK, T.F., SLUTSKER, I., TANRÉ, D., BUIS, J.P., SETZER, A., VERMOTE, E., REAGAN, J.A., KAUFMAN, Y.J., NAKAJIMA, T., LAVENU, F., JANKOWIAK, I. and SMIRNOV, A., 1998, AERONET—a federal instrument network and data archive for aerosol characterization. *Remote Sensing of Environment*, **66**, pp. 1–16.

HOLBEN, B.N., TANRE, D., SMIRNOV, A., ECK, T.F., SLUTSKER, I., ABUHASSAN, N., NEWCOMB, W., SCHAFER, J.S., CHATENET, B., LAVENU, F., KAUFMAN, Y.J., VANDE CASTLE, J., SETZER, A., MARKHAM, B., CLARK, D., FROUIN, R., HALTHORE, R., KARNIELI, A., O'NEILL, N.T., PIETRAS, C., PINKER, R.T., VOSS, K. and ZIBORDI, G., 2001, An emerging ground-based aerosol climatology: Aerosol Optical Depth from AERONET. *Journal of Geophysical Research*, **106**, pp. 12 067–12 097.

JUNGE, C.E., 1963, *Air Chemistry and Radioactivity*, 3rd edn (New York: Academic Press).

KLETT, J., 1985, Lidar inversion with variable backscatter/extinction ratios. *Applied Optics*, **24**, pp. 1638–1643.

LISTON, G.E. and PIELKE, R., 2001, A climate version of the regional atmospheric modelling system. *Theoretical Applied Climatology*, **68**, pp. 155–173.

MACCHIONE M., OLIVEIRA, A.P., GALLAFRIO, C.T., MUCHÃO, F.P., OBARA, M.T., GUIMARÃES, E.T., ARTAXO, P., KING, M., LORENZI-FILHO, G., JUNQUEIRA, V.C.B. and SALDIVA, P.H.N., 1999, Acute effects of inhalable particles on the frogs palate mucociliary epithelium. *Environmental Health Perspectives*, **107**, pp. 829–833.

MARENCO, F., SANTACESARIA, V., BAIS, A., BALIS, D., DI SARRA D., PAPAYANNIS, A. and ZEREFOS, C.S., 1997, Optical properties of tropospheric aerosols determined by lidar and spectrophotometric measurements (PAUR campaign). *Applied Optics*, **36**, pp. 6785–6886.

MEASURES, R., 1992, *Laser Remote Sensing*, 4th edn (New York: John Wiley).

MELFI, S., SPINHIRNE, J., CHOU, S.-C. and PALM, S., 1985, Lidar observations of vertically organized convection in the planetary boundary layer over the ocean. *Journal of Climate and Applied Meteorology*, **24**, pp. 806–821.

MENUT, L., FLAMANT, C., PELON, J. and FLAMANT, P.H., 1999, Urban boundary-layer height determination from lidar measurements over the Paris area. *Applied Optics*, **38**, pp. 945–954.

Downloaded by [USP University of Sao Paulo] at 08:21 30 April 2013

MÜLLER, D., WANDIGER, U., ALTHAUSEN, D., MATTIS, I. and ANSMANN, A., 1998, Retrieval of physical properties from lidar observations of extinction and backscatter at multiple wavelengths. *Applied Optics*, **37**, pp. 2260–2263.

MULLER, D., FRANKE, K., WAGNER, F., ALTHAUSEN, D., ANSMANN, A., HEINTZENBERG, J. and VERNER, G., 2001, Vertical profiling of optical and physical particle properties over the tropical Indian Ocean with six-wavelength lidar. 2, case studies. *Journal of Geophysical Research*, **595**, pp. 28577–28595.

PANDIS, S.N., WEXLER, A.S. and SEINFELD, J.H., 1995, Dynamics of tropospheric aerosols. *Journal of Physical Chemistry*, **99**, pp. 9646–9659.

PAPAYANNIS, A. and BALIS, D., 1998, Study of the structure of the lower troposphere over Athens using a backscattering lidar during the MEDCAPHOT-TRACE experiment: measurements over a suburban area. *Atmospheric Environment*, **32**, pp. 2161–2172.

PAPAYANNIS, A. and CHOURDAKIS, G., 2002, The EOLE Project. A multi-wavelength laser remote sensing (lidar) system for ozone and aerosol measurements in the troposphere and the lower stratosphere. Part II: Aerosol measurements over Athens, Greece. *International Journal of Remote Sensing*, **23**, pp. 179–196.

PAPAYANNIS, A., ANCELLET, G., PELON, J. and MEGIE, G., 1990, Multi-wavelength lidar for ozone measurements in the troposphere and the lower stratosphere. *Applied Optics*, **29**, pp. 467–476.

PAVLOW, M., KOVALEV, V., ANSMANN, A. and HELMERT, K., 2004, Iterative determination of the aerosol extinction coefficient profile and the mean extinction-to-backscatter ratio from multiangle lidar data. *Proceedings of the 22nd International Laser Radar Conference*, ESA SP-561, G. Pappalardo and A. Amodeo (Eds), pp. 491–494.

PIELKE, R.A., COTTON, W.R., WALKO, R.L., TREMBACK, C.J., LYONS, W.A., GRASSO, L.D., NICHOLLS, M.E., MORAN, M.D., WESLEY, D.A., LEE, T.J. and COPELAND, J.H., 1992, A comprehensive meteorological modeling system—RAMS. *Meteorology and Atmospheric Physics*, **49**, pp. 69–91.

SALDIVA, P.H.N., POPE, C.A., SCHWARTZ, J., DOCKERY, D.W., LICHTENFELS, A.J., SALGE, J.M., BARONE, I. and BOHM, G.M., 1995, Air pollution and mortality in elderly people: a time-series study in São Paulo, Brazil. *Archives of Environmental Health*, **50**, pp. 159–163.

SASANO, Y., SHIMIZU, H., TAKEUCHE, N. and OKUDA, N., 1979, Geometrical form factor in the laser–radar equation-experimental-determination. *Applied Optics*, **18**, pp. 3908–3910.

STULL, R.B., 1991, *An Introduction to Boundary Layer Meteorology*, 2nd edn (Boston: Kluwer Academic).

TAKAMURA, T., SASANO, Y. and HAYASAKA, T., 1994, Tropospheric aerosol optical properties derived from lidar, sun photometer, and optical particle counter measurements. *Applied Optics*, **33**, pp. 7132–7140.

TATARO, B., SUGIMOTO, N. and SHIMIZY, A., 2004, Systematic observations of lidar ratio for tropospheric aerosols and clouds by high-spectral-resolution lidar over Tsukuba, Japan. *Proceedings of the 22nd International Laser Radar Conference*, ESA SP-561, G. Pappalardo and A. Amodeo (Eds), pp. 329–332.

WANDIGER, U., MULLER, D., BOECKMANN, C., ALTHAUSEN, D., MATTHIAS, V., BOESENBERG, J., WEIB, B., FIEBIG, M., WENDISCH, M., STOHL, A. and ANSMANN, A., 2002, Optical and physical characterization of biomass burning and industrial pollution aerosols from multiwavelength lidar and aircraft measurements. *Journal of Geophysical Research*, **107**, DOI 10.1029/2000, ID000202.

WELTON, E.J., VOSS, K.J., QUINN, P.K., FLATAU, P.J., MARKOWICZ, K., CAMPBELL, J.R., SPINHIRNE, J.D., GORDON, H.R. and JOHNSON, J.E., 2002, Measurements of aerosol vertical profiles and optical properties during INDOEX 1999 using micropulse lidars. *Journal of Geophysical Research*, **107**(D19), 8019, 10.1029/2000JD000038.

Downloaded by [USP University of Sao Paulo] at 08:21 30 April 2013